

Effects of moderate Damköhler number on miscible viscous fingering involving viscosity decrease due to a chemical reaction

YUICHIRO NAGATSU†, YUSUKE KONDO,
YOSHIHITO KATO AND YUTAKA TADA

Department of Materials Science and Engineering, Graduate School of Engineering, Nagoya
Institute of Technology, Gokiso-cho, Showa-ku, Nagoya, Aichi 466-8555, Japan

(Received 1 May 2008 and in revised form 28 November 2008)

We have succeeded in experimentally investigating the effects of a moderate Damköhler number, Da (defined as the ratio between a characteristic time of fluid motion and that of a chemical reaction), for various Péclet numbers, Pe , on miscible viscous fingering involving a decrease in the viscosity of the displaced liquid due to a chemical reaction in Hele-Shaw cells. We achieved this by using a chemical reaction between a polymer solution and metal ions. Main analysis has been done for the radial fingering. In the range of Pe employed here, the fingering patterns without the reaction ($Da = 0$) were independent of Pe . The fingering patterns with the reaction depended on the single parameter, Da , and the area occupied by the fingering pattern near the injection hole increased with Da in the range of Da employed here. The ratio of the area occupied by the fingering pattern within the circle radius of which is the length of longest finger to the area of the circle increased with Da in the range of Da employed here. This result is opposite to that of Nagatsu *et al.* (*J. Fluid Mech.*, vol. 571, 2007, p. 475), in which the area was decreased by the reaction decreasing the viscosity involving significantly high Da . Experiments in the linear geometry show that the shape of a single finger also depended on the single parameter, Da , and the finger width increased near the base with Da . This result is also opposite to that in the previous case in which the width of a single finger was considered to be decreased by the reaction. These results, interestingly, show that the effects of the decrease in the displaced liquid's viscosity due to chemical reaction on the fingering pattern for moderate Da are opposite to those for significantly high Da . A mechanism for the opposite effects on the fingering pattern depending on Da is discussed.

1. Introduction

When a more viscous fluid is displaced by a less viscous one in porous media and in Hele-Shaw cells, the interface or boundary of the two fluids becomes unstable and forms a finger-like pattern. This phenomenon is referred to as viscous fingering. Since the appearance of the pioneering works on the fluid mechanics of viscous fingering, published in the 1950s (Hill 1952; Saffman & Taylor 1958), many experimental and theoretical studies have been performed and some review articles have been published (Homsy 1987; McCloud & Maher 1995; Tanveer 2000). This issue regarding Newtonian fluids is well understood. There are two classes of viscous fingering: fingers formed in immiscible systems and those formed in miscible systems. The dimensionless

† Email address for correspondence: nagatsu@nitech.ac.jp

number that controls the fingering dynamics in immiscible systems is the capillary number Ca , which is defined as the ratio between viscous and interface-tension forces. In miscible systems, the dimensionless number is the Péclet number Pe , which is defined as the ratio between convective and diffusive transport rates of mass. For both systems, the nonlinear propagation of viscous fingering is governed by different mechanisms of shielding, spreading and splitting. Shielding is the phenomenon in which a finger slightly ahead of its neighbour fingers quickly outruns them and shields them from further growth. Spreading and splitting are the phenomena in which a finger that spreads until it reaches a certain width becomes unstable and splits (Homsy 1987).

Since the seminal work by Nittmann, Daccord & Stanley (1985) showing that viscous fingering patterns formed in a non-Newtonian fluid are quite different from those formed in Newtonian fluids, viscous fingering for non-Newtonian fluids has been paid special attention. Experiments in, for instance, clay slurries, colloidal fluids and polymer solutions have revealed branched fractal or fracture-like patterns (Nittmann *et al.* 1985; van Damme *et al.* 1986; Lemaire *et al.* 1991; Zhao & Maher 1993). The physical origin of the very different structures is so far unclear, mainly because these fluids can simultaneously display many non-Newtonian properties, such as shear thinning or thickening, viscoelasticity, yield stress, etc. Experiments have been performed within the last few years to disentangle the influence that different non-Newtonian flow properties have on the instability by using fluids that each exhibit only one non-Newtonian property, showing experimentally other non-Newtonian effects to be neglected (Lindner, Bonn & Meunier 2000; Vlad & Maher 2000; Lindner *et al.* 2002).

Recently, the effects of changes in a fluid's properties induced by chemical reactions between the more and less viscous liquids on the viscous fingering patterns have been investigated. DeWit & Homsy (1999*a*, 1999*b*) performed a numerical simulation on reactive miscible viscous fingering in porous media by assuming that the fluid's viscosity is given as a function of a chemical species concentration and by using a specific chemical kinetics. They found a new mechanism of viscous fingering that they call the 'droplet' mechanism, which involves the formation of isolated regions of either less or more viscous fluids in connected domains of the other. Fernandez & Homsy (2003) performed experiments on immiscible viscous fingering with a chemical reaction acting to reduce interfacial tension in a Hele-Shaw cell and found that the reaction made the fingers wider. They characterized the effects of the reaction on the reactive fingering pattern by the Damköhler number Da , which is defined as the ratio between a characteristic time of fluid motion and that of a chemical reaction. They showed that the effects of the reaction appeared only for intermediate Da , while the reactive fingering patterns were similar to that without the reaction for both small Da and high Da . Nagatsu *et al.* (2007) succeeded in experimentally showing how a reactive miscible viscous fingering pattern in a radial Hele-Shaw cell changed when the viscosity of the more viscous liquid was varied by instantaneous chemical reactions. This was done by making use of a polymer solution's dependence of viscosity on pH. In this case, instantaneous reactions meant that Da was significantly high or could be treated as infinity. When the viscosity was increased by the chemical reaction, the shielding effect (mentioned earlier) was suppressed and the fingers were widened. As a result, the ratio of the area occupied by the fingering pattern in a circle whose radius was the length of the longest finger was larger in the reactive case compared to the non-reactive case. When the viscosity was decreased by the chemical reaction, in contrast, the shielding effect was enhanced and the fingers were narrowed. These changes led to the area ratio being smaller in the reactive case than in the non-reactive one.

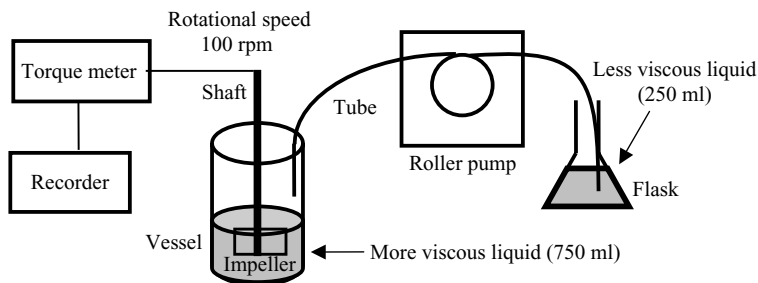


FIGURE 1. Experimental apparatus to measure the rate of the decrease in viscosity due to the reaction.

In the present study, we have found that a chemical reaction between a polymer solution and metal ions decreases the viscosity of the polymer solution. Additionally, we have found that the concentration of the metal ions changes the rate of the decrease in the viscosity, which corresponds to the chemical reaction rate, under the condition in which the rate is finite. We have experimentally investigated the effects of Da under the condition of finite Da on a miscible viscous fingering pattern in a radial Hele-Shaw cell involving a decrease in the more viscous liquid's viscosity due to chemical reaction by using a polymer solution as the more viscous liquid and a solution containing metal ions as the less viscous liquid. In addition, the experiments using a linear Hele-Shaw cell have been additionally performed to investigate the effects of the present reaction on a single finger.

The present article is organized as follows. Section 2 first describes a detail of the liquids and chemical reaction employed and next explains several parameters regarding the experiment on reactive miscible viscous fingering in the radial geometry. Section 3 describes visualization results of the radial fingering pattern and some quantitative characterizations of the pattern. Furthermore, the experiments regarding a single finger in the linear geometry are described in this section. Mechanism of the change in the fingering pattern by the present reaction is discussed in § 4. Finally, conclusion is given in § 5.

2. Experimental

2.1. Liquids and chemical reaction

In the present study, we have found that a chemical reaction between a polyethylene oxide (PEO) solution and a solution containing copper ions Cu^{2+} and ferrous ions Fe^{2+} decreases the viscosity of the mixture solution and that the concentration of the ions changes the rate of the decrease in the viscosity, which corresponds to the chemical reaction rate, under the condition in which the rate is finite. Here, the rate of the viscosity's decrease due to the chemical reaction was measured by using the experimental apparatus shown in figure 1. We regard torque imposed on a shaft involving an impeller required to agitate a solution in a vessel at a constant rotational speed as the indicator of the viscosity of the solution in the vessel. We used a cylindrical acrylic vessel with 130 mm inner diameter and a six-blade paddle impeller 100 mm in diameter and 60 mm tall. A total of 250 ml of the less viscous solution containing Cu^{2+} and Fe^{2+} at given concentrations was added for 40 s by a roller pump to the vessel in which the more viscous 0.67 wt % PEO solution with 750 ml was agitated by an impeller at 100 rpm. After the addition of the ionic solution, the concentration of the PEO in the solution in the vessel became 0.5 wt % and that of each type of ion became a quarter of the concentration of that ion type in the

	More viscous liquid	Less viscous liquid	κ (s ⁻¹)
Case (I)	0.67 wt % PEO solution	Deionized water	0
Case (II)	0.67 wt % PEO solution	CuCl ₂ 1.0 M + FeCl ₂ 1.0 M solution	0.011
Case (III)	0.67 wt % PEO solution	CuCl ₂ 5.0 M + FeCl ₂ 1.0 M solution	0.030
Case (IV)	0.67 wt % PEO solution	CuCl ₂ 3.0 M + FeCl ₂ 3.0 M solution	0.049

TABLE 1. Liquids used for the measurement of the rate of decrease in viscosity due to the reaction and the obtained first-order rate constant of the decrease, κ .

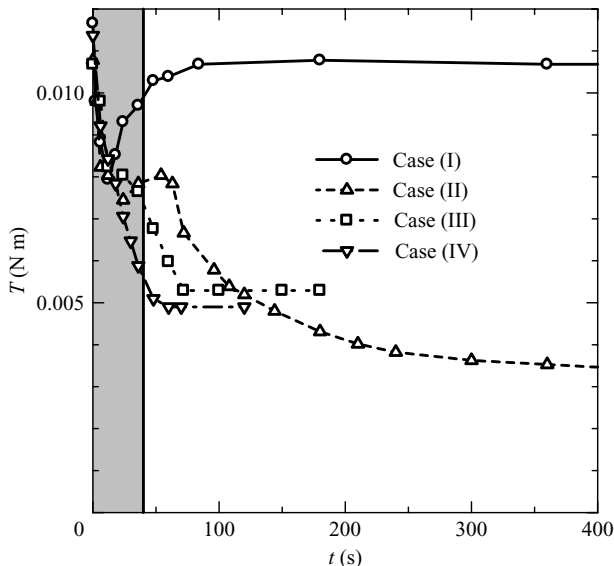


FIGURE 2. Time evolution of the measured torque during the decrease of viscosity due to the reaction. The grey region indicates the period of addition of the less viscous liquid.

added ionic solution. Agitation was kept constant at 100 rpm during and after the addition of the ionic solution. We measured the torque during and after the injection of the ionic solution using a torque meter. We used PEO the molecular weight of which is 5 million (Alfa Aesar). A mixture of copper chloride solution and ferrous chloride solution was used as the ionic solution. Four cases in which we varied the concentration of Cu^{2+} and Fe^{2+} were examined, as shown in table 1. Note that case (I) is a non-reactive case, which we used as a reference experiment for the reactive cases (II)–(IV).

Time evolutions of the measured torque, T , in the four cases are shown in figure 2, in which $t = 0$ s is taken to be the time when the less viscous solution begins to be added. In case (I), involving no metal ions, the torque decreases with time during the addition of the less viscous solution, while it increases with time from the halfway point of the addition, and finally it reaches a constant value. The torque's decrease and its following increase during the addition occurs for the following reason. Immediately after the start of the injection of the less viscous liquid, the less viscous liquid flows near the wall of the vessel and acts as a lubricant, which results in a decrease in the torque imposed on the shaft of the impeller required to agitate the solution at a constant rotational speed. As the less viscous liquid starts to mix with the more viscous liquid, the lubrication action gradually disappears, which leads to a renewed increase in the torque. In case (II), the torque's decrease during the addition and the

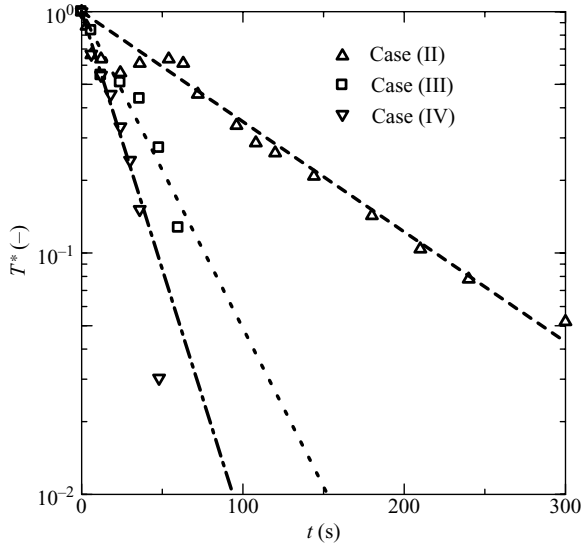


FIGURE 3. Time evolution of the normalized torque in a semi-logarithmic plot.

torque's increase immediately after the addition occur as in case (I), while the torque decreases again after the temporal increase in the torque. The torque's decrease after the completion of the addition is caused by the decrease in the solution's viscosity due to a chemical reaction between the PEO solution and the metal ions. Finally, the torque reaches a constant value. In cases (III) and (IV), because of the torque's decrease due to the addition of the less viscous solution plus the relatively faster rate of the viscosity's decrease due to the relatively faster reaction, the torque monotonically decreases with time and finally reaches a constant value. The time required until the torque finally reaches a constant value becomes shorter in the order of cases (IV), (III) and (II), which indicates that the chemical reaction rate is larger in the order of these cases. Note that our viscosity measurement by a rotational viscometer confirmed that the viscosity of the solution in the vessel after the completion of the addition of the ionic solution finally became that of water for cases (II)–(IV). These results show that the difference in the concentrations of the metal ions employed in the present study induces the rate of the viscosity's decrease but does not induce the extent of the viscosity's decrease. Also note that the constant value the torque finally reaches is somewhat larger in cases (III) and (IV) than in case (II). This is considered to be due to the density of the mixture being larger in cases (III) and (IV) than in case (II).

We normalize the decrease in the torque by the difference between the initial value T_0 and the final value T_∞ , which is denoted as T^* , as follows:

$$T^* = \frac{T - T_\infty}{T_0 - T_\infty}.$$

As shown in figure 3, the decrease in the reduced torque exhibits a single exponential decay. The slope gives the first-order rate constant of the viscosity's decrease due to the chemical reaction, κ . The obtained values of κ in cases (II)–(IV) are shown in table 1. This procedure is essentially the same as that employed by Fernandez & Homsy (2003). It can be confirmed that κ is larger in the order of cases (IV), (III) and (II).

	More viscous liquid	Less viscous liquid	κ (s ⁻¹)
Case (A)	1.0 wt % PEO solution	Deionized water	0
Case (B)	1.0 wt % PEO solution	CuCl ₂ 0.5 M + FeCl ₂ 0.5 M solution	0.011
Case (C)	1.0 wt % PEO solution	CuCl ₂ 2.5 M + FeCl ₂ 0.5 M solution	0.030
Case (D)	1.0 wt% PEO solution	CuCl ₂ 1.5 M + FeCl ₂ 1.5 M solution	0.049

TABLE 2. Liquids used for the viscous fingering experiment and the first-order rate constant of the decrease in viscosity due to the reaction, κ .

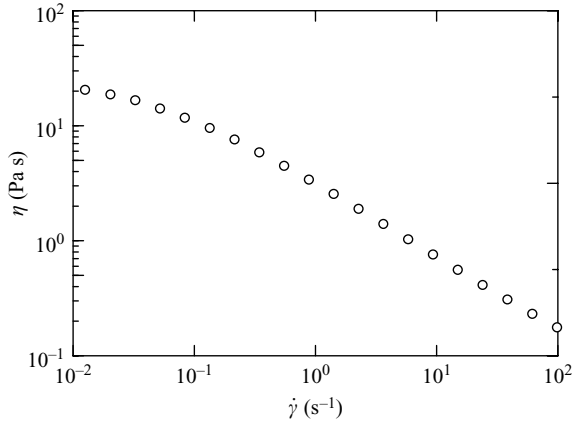


FIGURE 4. Steady shear viscosity, η , of 1.0 wt % PEO solution with the blue dye.

2.2. On viscous fingering experiments

A viscous fingering experiment was performed by using the combination of the more and less viscous liquids shown in table 2. It is reasonable to regard the average concentrations of PEO and metal ions in the boundary region between the more viscous PEO solution and the less viscous ionic solution as the half values of the initial concentration of PEO in the more viscous liquid and that of metal ions in the less viscous liquid. The average concentrations of PEO and metal ions in the boundary region in cases (A)–(D) in the viscous fingering experiment are the same as the concentration of PEO and metal ions in the vessel after the addition of the less viscous liquid in the experiment in which we measured the rate of decreasing viscosity due to the reaction. Thus, the values of κ obtained in the case of (I)–(IV) in the torque experiment were used as the rate of viscosity's decrease due to the reaction in cases (A)–(D), respectively.

It is customary to dye the less viscous liquid in viscous fingering experiments where both the less and more viscous fluids are liquids. In the present study, however, the more viscous liquid, i.e. the 1.0 wt % PEO solution, was dyed blue with methylene blue because it was difficult to find dyes for the solution containing Cu²⁺ and Fe²⁺. The concentration of the methylene blue was set as 0.1 wt %. We used a rheometer (HAAKE RS600) to measure the steady shear viscosity, η , and the steady first normal stress difference (which corresponds to the elastic property), N_1 , of the 1.0 wt % PEO solution with the dye. The measurement result is shown in figure 4. The steady shear viscosity shows shear-thinning behaviour. No measurable value of N_1 was found in the range of $\dot{\gamma}$ tested (up to 100 s⁻¹), and thus it does not appear in figure 4. This

result indicates that elastic effects are negligible for the PEO solution used in the viscous fingering experiment in the range of $\dot{\gamma} < 100 \text{ s}^{-1}$. As mentioned later, in the present viscous fingering experiments the shear rate in the vicinity of the fingertip was significantly less than 100 s^{-1} . Therefore, the elastic property of the PEO solution is negligible in the present study, although elastic effects are known to influence the viscous fingering pattern, as mentioned in the § 1.

The viscous fingering experiments were conducted using radial and linear Hele-Shaw cells. Since analysis of the experiments has been performed mainly for the radial geometry, we explain only the experiments in the radial geometry in this section. The description of the experiments in the linear geometry will be made in § 3.5. The experimental set-up was the same as that used in our previous study (Nagatsu *et al.* 2007). In the present study, the gap width b is set as $b = 0.5 \text{ mm}$. The bulk finger advancement velocity, U , is defined in (2.1) as well as in Nagatsu *et al.* (2007), as follows:

$$U = \frac{q}{2\pi Rb}, \quad (2.1)$$

where q is the volumetric flow rate of the injection of the less viscous liquid. This indicates the increase rate of the circle's radius, R , when the less viscous liquid completely displaces the more viscous liquid, keeping the boundary between the two liquids circular. The Péclet number, Pe , is as defined in (2.2) as well as in Nagatsu *et al.* (2007), as follows:

$$Pe = \frac{RU}{D} = \frac{q}{2\pi bD}, \quad (2.2)$$

where D is the diffusion coefficient between the more and less viscous liquids. In the present study, D can be regarded as the diffusion coefficient of the polymer at small concentrations in water, because the more viscous liquid is 1.0 wt % PEO solution and the less viscous liquid is aqueous solution, and so D is estimated to be $1 \times 10^{-9} \text{ m}^2 \text{ s}^{-1}$ (Nagatsu *et al.* 2007). From (2.2), we see that Pe is proportional to U , and thus in the present study it is used as a parameter indicating the bulk finger advancement velocity. Because b is constant here, Pe is also proportional to q .

As in Nagatsu *et al.* (2007), the shear rate in the vicinity of the fingertip, $\dot{\gamma}_f$, is roughly estimated in (2.3) as follows:

$$\dot{\gamma}_f = \frac{U}{b/2} = \frac{q}{\pi Rb^2}. \quad (2.3)$$

From (2.1), U is largest at the injection hole, at $R = 2 \text{ mm}$ (the radius of the injection hole for liquids in the Hele-Shaw cell is 2 mm). In the present experiments, we examined the condition of $\dot{\gamma}_f$ at $R = 2 \text{ mm}$ in the range of $0.41 \text{ s}^{-1} \leq \dot{\gamma}_f \leq 4.1 \text{ s}^{-1}$, resulting in negligible elastic effects. This condition corresponds to $2.0 \times 10^2 \leq Pe \leq 20 \times 10^2$ in terms of Pe .

We define the characteristic time as the nominal residence time of fluid t_r . As found in Fernandez & Homsy (2003)

$$t_r = \frac{bR_0^2}{2q}. \quad (2.4)$$

Although Fernandez & Homsy (2003) set R_0 as the radius of the cell, we set $R_0 = 58 \text{ mm}$, because our cell was not formed by circular plates but by square plates. The reason for our choice of 58 mm is explained later. The Damköhler number Da , which is the ratio of the residence time of fluid to the characteristic time of the

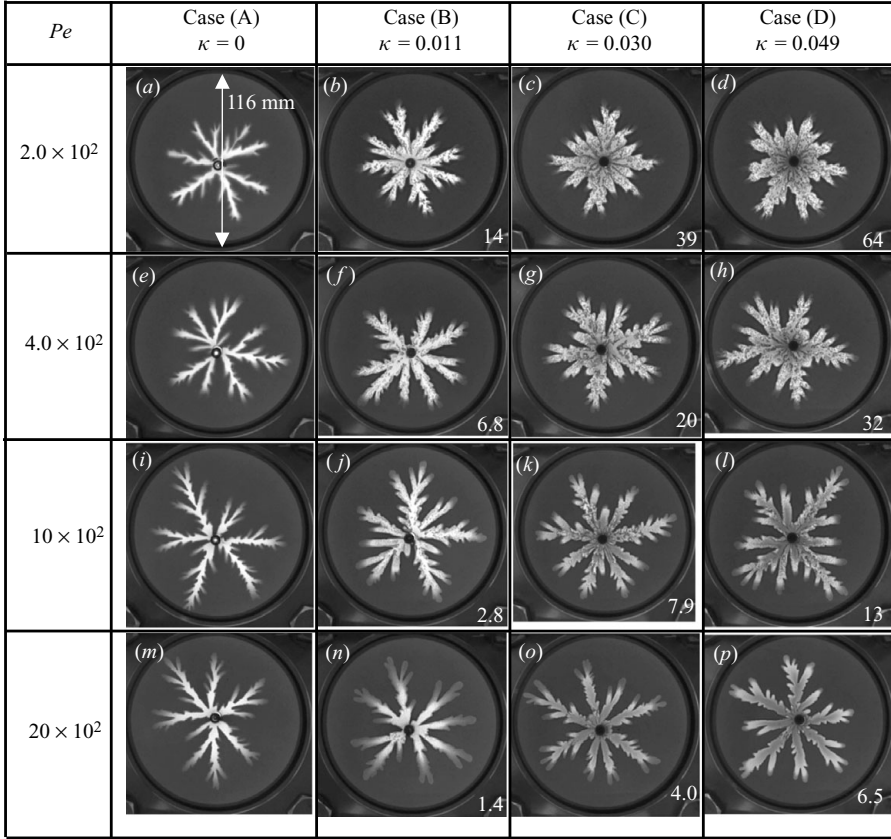


FIGURE 5. Miscible viscous fingering patterns for various Pe and for cases (A)–(D), where the amount of injected less viscous liquid is constant ($qt = 7.7 \times 10^{-7} \text{ m}^3$, where t is the injection time of the less viscous liquid). The value of Da is shown in the lower right of each image. The injection time, t , is $t = 1200, 600, 240$ and 120 s for $Pe = 2.0 \times 10^2$, $Pe = 4.0 \times 10^2$, $Pe = 10 \times 10^2$ and $Pe = 20 \times 10^2$, respectively.

reaction, is defined as (2.5) as well as in Fernandez & Homsy (2003), as follows:

$$Da = \frac{\kappa b R_0^2}{2q}. \quad (2.5)$$

In the present study, Da was widely varied from 1.4 to 64 in the reactive cases. Note that $Da = 0$ in the non-reactive case.

3. Results

3.1. Fingering patterns for various Pe and Da under the condition of a set amount of injected less viscous liquid

Figure 5 shows miscible viscous fingering patterns in cases (A)–(D) for various Pe in which the total amount of the injected less viscous liquid is always the same ($qt = 7.7 \times 10^{-7} \text{ m}^3$, where t is the injection time of the less viscous liquid). The value of Da is shown in the lower right corner of each image. In case (A) (the non-reactive case), no significant effects of Pe on the fingering pattern were observed in the range of Pe tested. In the reactive cases (B)–(D), the finger width around the finger tip seemed to be slightly widened for each Pe . Significant effects of the reaction on the pattern appeared in the region around the injection hole. The area occupied by the

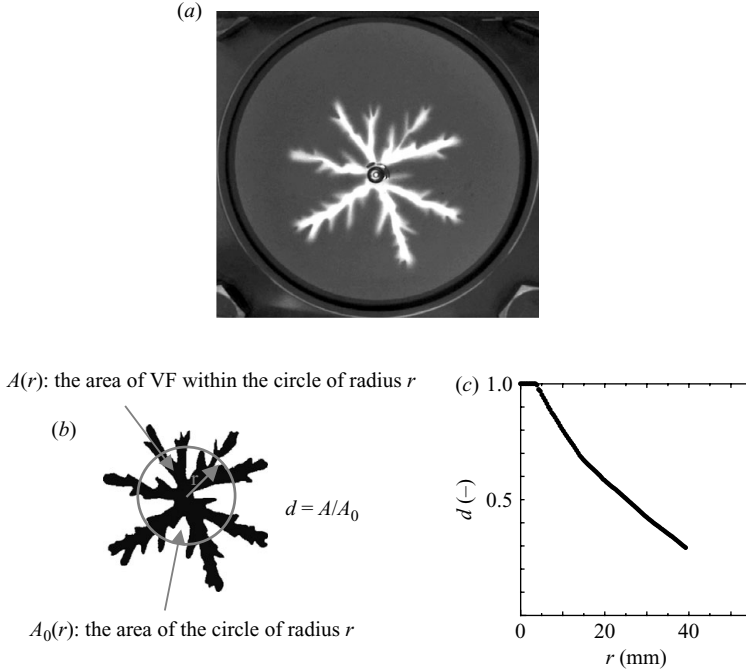


FIGURE 6. Example of the d - r curve. (a) Photograph of the fingering pattern. (b) The extracted image of the fingering pattern from figure (a) by image analysis and the definition of the area density of the fingering pattern, d . Here the area occupied by the fingering pattern within an arbitrary radius r and the area of the circle of radius πr^2 are denoted as $A(r)$ and $A_0(r)$, respectively. (c) The d - r curve for the fingering pattern in figure (b).

fingering pattern around the injection hole increased with κ for each Pe and with a decrease in Pe for each κ . These results show that the area occupied by the pattern around the injection hole increased with Da for each Pe or for each κ . As mentioned above, the patterns are independent of Pe in the non-reactive case in the range of Pe tested. This suggests that the fingering pattern depends only on the single parameter, Da . Indeed, similar Da gives similar finger patterns. We can see similar patterns in (c) and (h) ($Da = 32 - 39$), in (b), (g) and (l) ($Da = 13 - 20$), in (f), (k) and (p) ($Da = 6.5 - 7.9$) or in (j) and (o) ($Da = 2.8 - 4.0$). Note that R_0 is set to 58 mm in the present study because the inner diameter of the flange is 116 mm (and thus the radius is 58 mm), as shown in figure 5(a).

In the present study, the concept of area density proposed by Chen (1989) was used to quantitatively evaluate the fingering patterns. An example is shown in figure 6. The fingering pattern was extracted from the photograph by an image analysis system (figures 6a and 6b). We measured the area density of the fingering pattern, d , which is defined as the ratio of the area occupied by the fingering pattern, $A(r)$, within an arbitrary radius r to the area of the circle of the radius, $A_0(r) = \pi r^2$ (figure 6b). We plotted d versus r (figure 6c). The d - r curve and other quantitative estimation described hereafter are the average of two experiments for each experimental condition.

Figure 7 shows the effects of Pe on the d - r curves of the fingering pattern shown in figure 5 for cases (A)–(D). In the non-reactive case (A), we can confirm that the d - r curves are independent of Pe . In the reactive cases (B)–(D), d around the injection

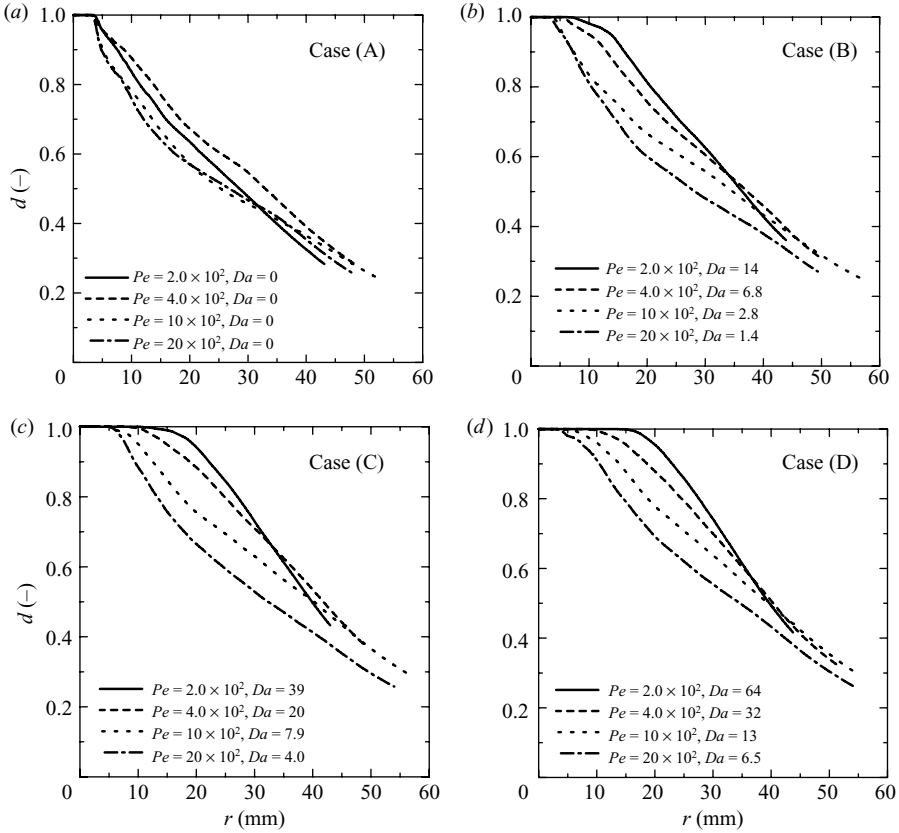


FIGURE 7. Effects of Pe on the d – r curve for cases (A)–(D) regarding the fingering patterns shown in figure 5.

hole ($r \approx 20$ mm) increases with a decrease in Pe , although the difference in d becomes small in the region of large r ($r \approx 40$ mm). Figure 8 shows the effects of κ on the d – r curves for various Pe . For each Pe , d increases with κ for any r in the range in which the pattern is present, although the difference between cases (C) and (D) is slight. The increase in d with κ is more pronounced around the injection hole ($r \approx 20$ mm), while the difference in d becomes small in the region of large r ($r \approx 40$ mm) (regarding this, more discussion will be made in §3.4). In other words, figures 7 and 8 show that d around the injection hole ($r \approx 20$ mm) increases with Da for each Pe or for each κ . Figure 9 shows the d – r curves in the reactive cases in terms of Da . Here, the d – r curves of similar values of Da are drawn with the same colour. In each colour, Da is high in the order of the solid, broken and dotted lines. As shown, the curves of the same colour roughly coincide. This shows that the configurations of the d – r curve depend on Da and are independent Pe . These results shown in figures 7–9 indicate that the observation results shown in figure 5 can be quantitatively confirmed by the d – r curves.

To quantitatively evaluate the extent of the increase in the area occupied by the fingering pattern around the injection hole, we measured the area density of the pattern at $r = 20$ mm in the fingering pattern shown in figure 5, d_{20} , which is the ratio of the area occupied by the fingering pattern within $r < 20$ mm to the area of the circle with a radius of 20 mm. Figure 10 shows the relationship between d_{20} and Da . As shown, d_{20} depends on the single parameter Da for various Pe and κ and increases

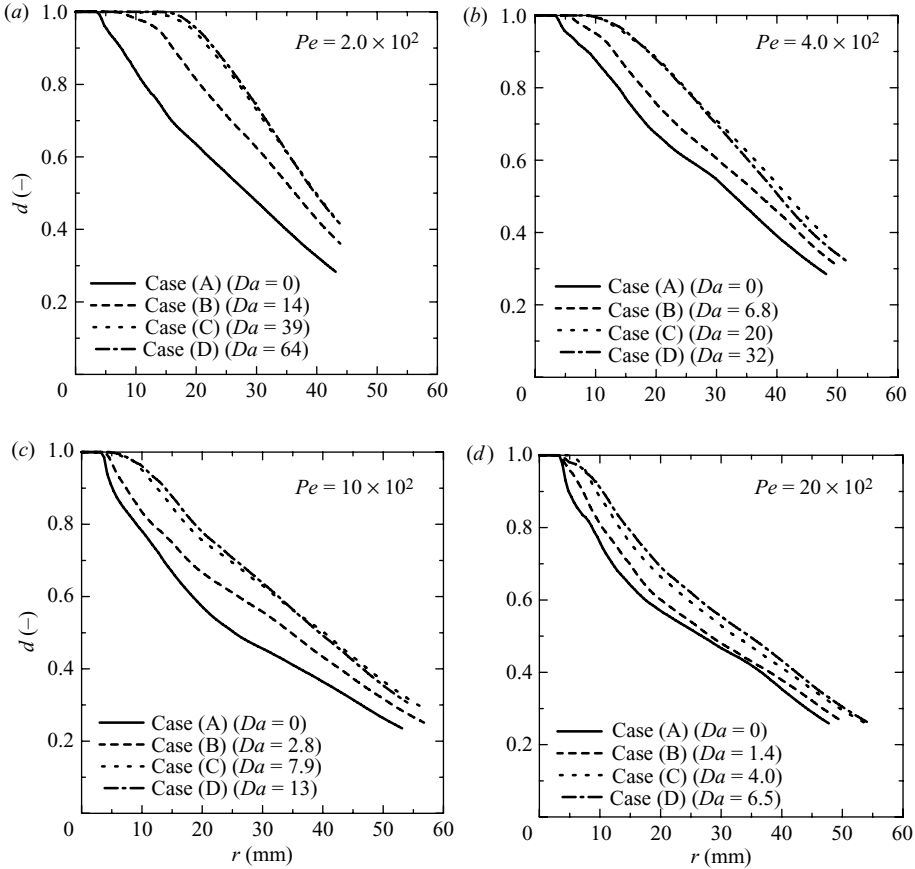


FIGURE 8. Effects of κ on the d - r curve for various Pe regarding the fingering patterns shown in figure 5.

with Da . The dependence of d_{20} on the single parameter Da is considered to be caused by the d - r curves being independent of Pe for the non-reactive cases in the present experimental condition.

We measure the fractal dimension, d_f , of the whole fingering pattern shown in figure 5 using the box counting method (Vicsek 1989; Fernandez & Homsy 2003). Results are shown in figure 11. We find that d_f also scales with Da and increases with Da .

3.2. Effects of Da on the time evolution of the reaction's influence on the fingering pattern

In the present study, it is important to investigate how the effects of the reaction on the fingering pattern change with time, since the chemical reaction rate is finite. Time evolutions of the effect of the reaction for low Da and high Da are displayed in figures 12 and 13, respectively. Figures 12(a) and 12(b) are the photographs of time evolution of the fingering pattern for $Da=0$ (no reaction) and $Da=6.5$ for $Pe=20 \times 10^2$. Figure 12(c) shows the d - r curves (plots) of the fingering patterns shown in figures 12(a) and 12(b). In the early stage ($t=10$ s), a difference between the patterns and the d - r curves without and with the reaction was hardly observed. In the middle stage ($t=60$ s), a slight difference between them appeared, and in the later stage ($t=120$ s), the difference between them was more pronounced. It should be noted that

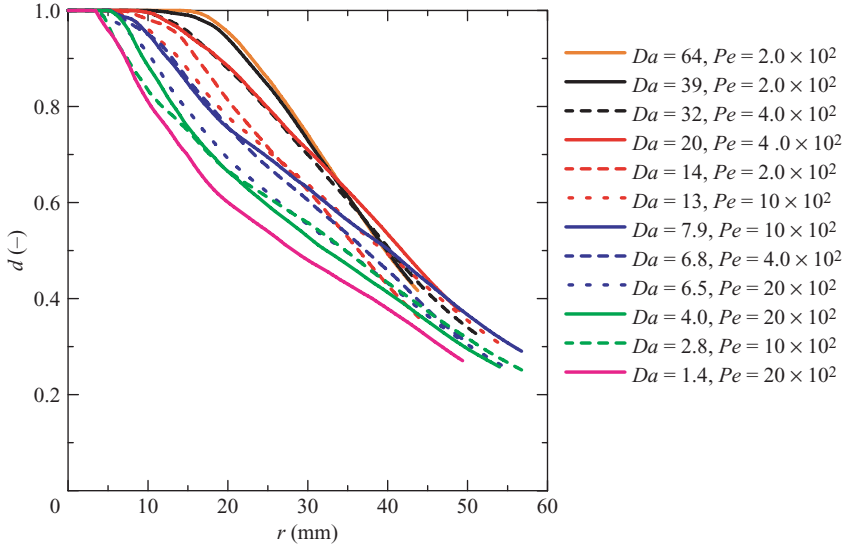


FIGURE 9. The $d-r$ curves for various values of Da regarding the fingering patterns shown in figure 5.

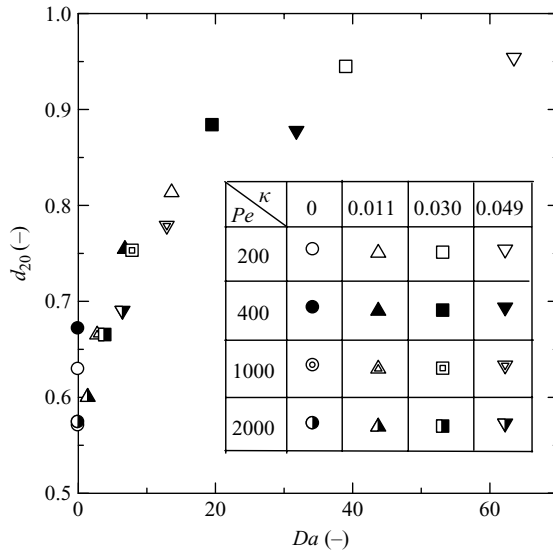


FIGURE 10. Relationship between d_{20} and Da regarding the fingering patterns shown in figure 5.

in the middle and later stages the $d-r$ curves around the injection hole ($r \approx 20$ mm) in the non-reactive case hardly change, while those in the reactive case increase with time. Figures 13(a) and 13(b) are the photographs of time evolution of the fingering pattern for $Da = 0$ (no reaction) and $Da = 64$ for $Pe = 2.0 \times 10^2$. Figure 13(c) shows the $d-r$ curves (plots) of the patterns in figures 13(a) and 13(b). In the early stage ($t = 100$ s), a slight difference was observed. For high Da , a significant difference was observed in the middle stage ($t = 600$ s), and in the later stage ($t = 1200$ s), their difference was more pronounced. The results in figures 12 and 13 show that the influence of the

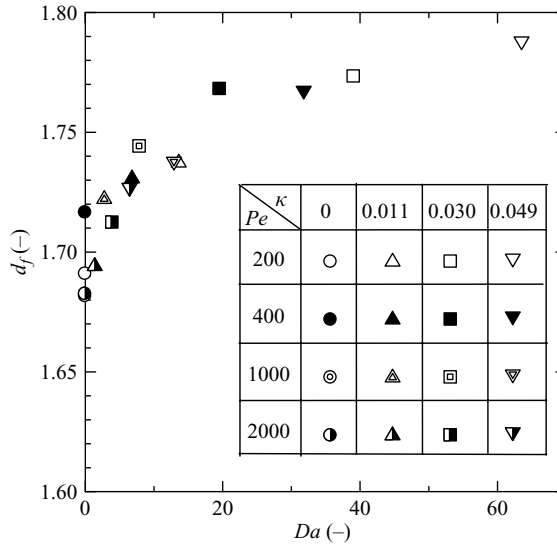


FIGURE 11. Fractal dimension, d_f , versus Da regarding the whole fingering patterns shown in figure 5.

reaction of the fingering pattern appears earlier for high Da than for low Da during fingering pattern formation. In the range of the present experimental conditions, the significant influence of the reaction on the pattern appears beginning in the later stage for low Da , while it appears beginning in the middle stage for high Da .

3.3. Area density of the fingering pattern under the condition of a constant length of the longest finger

In our previous study (Nagatsu *et al.* 2007), the area density of the fingering pattern, d_a , was defined as the ratio of the area occupied by the pattern within the circle with a radius r_{max} (r_{max} is defined as the length of the longest finger in each fingering pattern) to the area of the circle, πr_{max}^2 , and was employed as a quantitative evaluation of the fingering pattern. In the present study, the area density d_a in Nagatsu *et al.* (2007) is denoted as d_{max} . Figure 14 shows the relationship between d_{max} and Da in which $r_{max} = 40$ mm (in Nagatsu *et al.* (2007), $r_{max} = 37$ mm was mainly employed). Note that in this case the injection time of the less viscous liquid is not the same in each case. As shown, d_{max} increased with Da . In other words, d_{max} with the reaction is larger than that without the reaction in the range of Da employed here. It should be emphasized that in the previous study (Nagatsu *et al.* 2007) we showed that the decrease in the viscosity of the more viscous liquid induced by the instantaneous reaction (Da is sufficiently high) decreased d_{max} . The findings of the current and previous studies, interestingly, show that the effects of the decrease in the viscosity of the more viscous liquid due to chemical reaction on the viscous fingering pattern for moderate Da are opposite to those for significantly high Da . In other words, these effects depend on Da .

3.4. Comparison between the increase in d_{max} by the reaction decreasing viscosity with moderate Da and that by the reaction increasing viscosity with significantly high Da

In the previous study (Nagatsu *et al.*, 2007), we showed that the increase in the viscosity of the more viscous liquid induced by the instantaneous reaction increased d_{max} . In the present study, we attempt to quantitatively compare an increase in

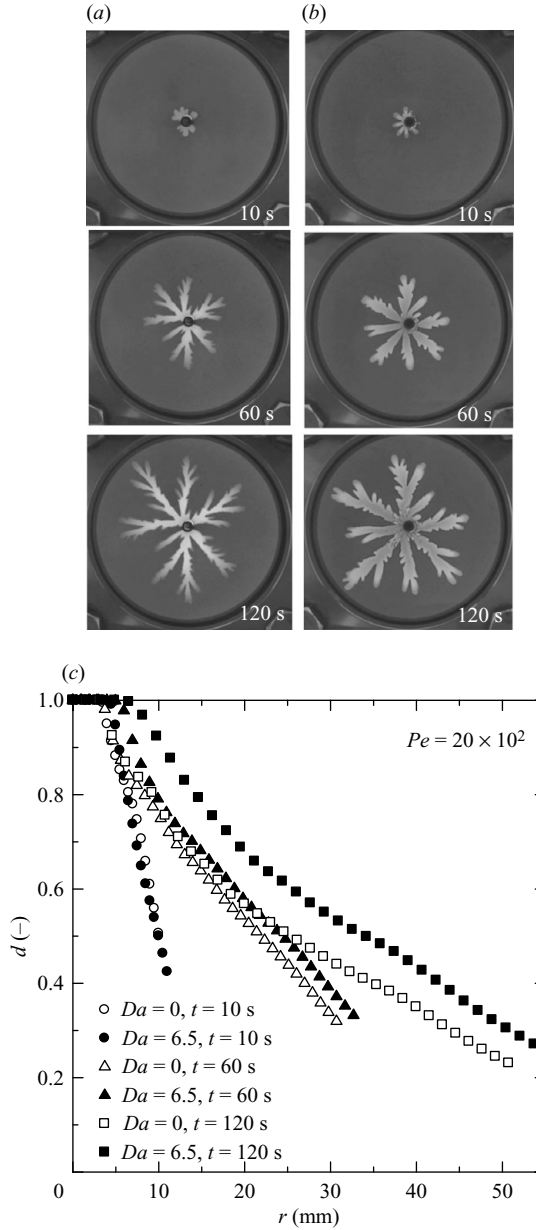


FIGURE 12. Time evolution of the fingering pattern for low Da . The photographs of time evolution of the fingering pattern for (a) $Da=0$ (no reaction) and (b) $Da=6.5$ for $Pe=20 \times 10^2$. The injection time is shown in the lower right of each image. (c) The $d-r$ curves (plots) of the fingering patterns shown in (a) and (b).

the area of the fingering pattern by the present reaction decreasing the viscosity involving moderate Da with that by the reaction increasing the viscosity involving significantly high Da . Here, we denote the difference between d without reaction and that with reaction as Δd . Figure 15(a) shows the typical $d-r$ curves (plots) for the present system and for the previous system involving the viscosity increase under the condition of $r_{max}=40$ mm. Figure 15(b) shows the $\Delta d-r$ curves obtained from the data in figure 15(a). Here, we employ the cases shown in figures 5(a) (without

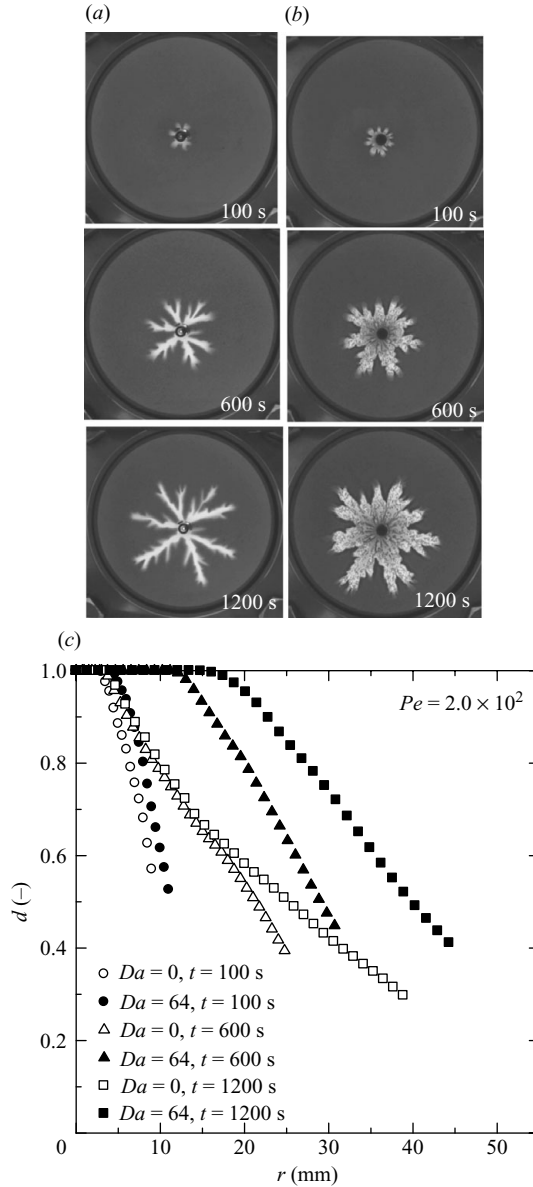


FIGURE 13. Time evolution of the fingering pattern for high Da . The photographs of time evolution of the fingering pattern for (a) $Da=0$ (no reaction) and (b) $Da=64$ for $Pe=2.0 \times 10^2$. The injection time is shown in the lower right of each image. (c) The d - r curves (plots) of the fingering patterns shown in (a) and (b).

reaction) and 5(c) (with reaction) for the present system and the cases shown in figures 5(a) (without reaction) and 5(b) (with reaction) in Nagatsu *et al.* (2007) for the previous system. In the previous case, Δd increases with r until $r \approx 30$ mm and slightly decreased for $r > 30$ mm. In the present system, Δd takes a maximum at $r \approx 20$ mm and significantly decreases for $r > 20$ mm. These results indicate that the effects of reaction significantly appear around the injection hole ($r < 20$ mm) in the present system, while these appear in the whole fingering pattern in the previous system.

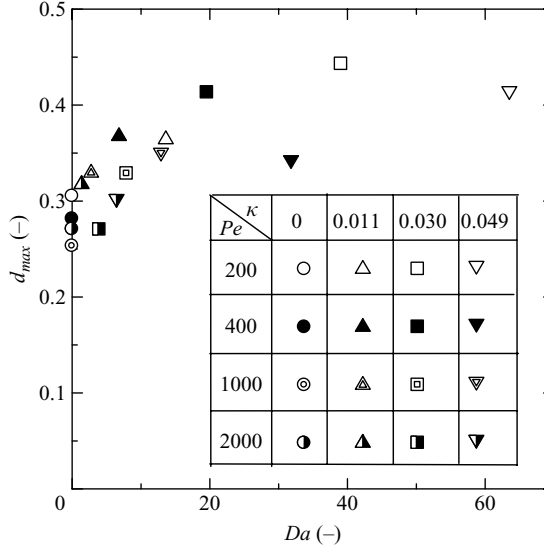


FIGURE 14. Relationship between d_{max} and Da under the condition of $r_{max} = 40$ mm.

The comparison is made by another way. Here, we introduce a new parameter, $\Delta A(r)$, defined as $\Delta A(r) = A(r + \Delta r) - A(r)$, where $A(r)$ is the area of the fingering pattern within radius r as mentioned earlier (see figure 6). We can examine where a change in the area of the fingering pattern by reaction significantly occurs by comparing $\Delta A(r) - r$ relation in the non-reactive case with that in the reactive case. Figure 16 shows $\Delta A(r)$ versus r for the present system (the cases shown in figures 5a (without reaction) and 5c (with reaction)) and for the previous system (the cases shown in figures 5a (without reaction) and 5b (with reaction) in Nagatsu *et al.* (2007)) under the condition of $r = 40$ mm. Here, Δr is set to 0.4 mm. In the previous system, the difference in $\Delta A(r)$ by the reaction is significant in the region of $8 \text{ mm} < r < 40 \text{ mm}$. In the present system, in contrast, the difference is significant only in the region of $8 \text{ mm} < r < 30 \text{ mm}$. It should be emphasized that little difference is observed in the region of $30 \text{ mm} < r < 40 \text{ mm}$. Note that the whole area is occupied by the fingering pattern in the region of small r ($r < 8 \text{ mm}$) for all cases. These results show that the area of the fingering pattern is increased in the whole fingering by the previous reaction; on the other hand, the present reaction increases the area mainly around the injection hole and does not increase the area around the finger tips.

In terms of the effects of the reaction on a single finger, we considered that the finger was totally widened (which means the finger was widened both near the base and near the tip) by the previous reaction. On the basis of the results in figures 15 and 16, we can consider that the finger is widened mainly near the base by the present reaction in terms of change in a single finger. The finger widening near the base is considered to lead to the increase in the area occupied by the radial fingering pattern around the injection hole.

3.5. Single-finger experiments

In the present study, to obtain direct information regarding the finger width and to answer our consideration mentioned in the preceding section in which the present reaction widens the finger mainly near the base, the experiments where a single finger linearly grows have been additionally performed. In these experiments, the cell's gap

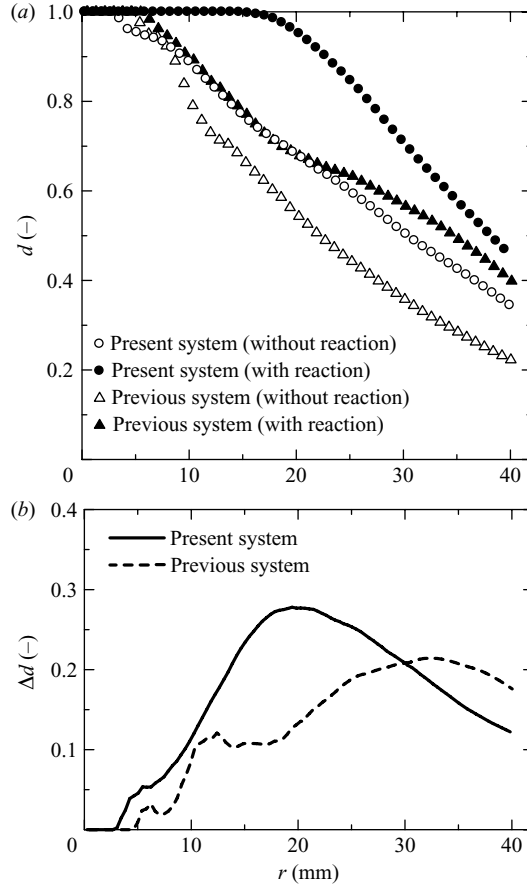


FIGURE 15. (a) Typical d - r curves (plots) for the present system and for the previous system involving the viscosity increase under the condition of $r_{max} = 40$ mm. (b) Δd - r curves obtained from the data in (a).

was also set to be $b = 0.5$ mm by placing a U-shaped silicone rubber between the two glass plates. The width and the length of the linear cell were set to be $w = 4$ mm and $l = 58$ mm, respectively. In the linear geometry, the finger advancement velocity, U , the Péclet number, Pe and the shear rate in the vicinity of the fingertip, $\dot{\gamma}_f$, are defined as, respectively,

$$U = \frac{q}{wb}, \quad (3.1)$$

$$Pe = \frac{lU}{D} = \frac{ql}{wbD}, \quad (3.2)$$

$$\dot{\gamma}_f = \frac{U}{b/2} = \frac{2q}{wb^2}. \quad (3.3)$$

Here, we examined the condition of $\dot{\gamma}_f$ in the range of $0.18 \text{ s}^{-1} \leq \dot{\gamma}_f \leq 1.8 \text{ s}^{-1}$, resulting in negligible elastic effects. This condition corresponds to $2.7 \times 10^3 \leq Pe \leq 27 \times 10^3$ in terms of Pe . The characteristic time as the nominal residence

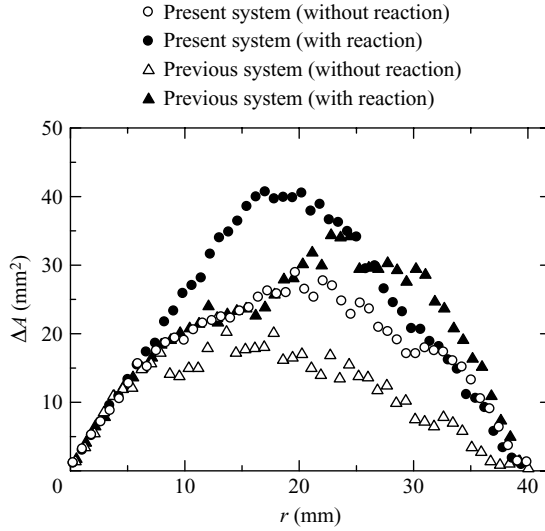


FIGURE 16. $\Delta A(r)$ as function of r under the condition of $r_{max} = 40$ mm for the present system and for the previous system.

time of fluid, t_r , and the Damköhler number, Da , are defined as, respectively,

$$t_r = \frac{wbl}{q}, \quad (3.4)$$

$$Da = \frac{\kappa wbl}{q}. \quad (3.5)$$

In the present study, Da was varied from 1.3 to 62 in the reactive cases.

Figure 17 shows the single fingers in cases (A)–(D) for various Pe in which the total amount of the injected less viscous liquid is always the same ($qt = 3.7 \times 10^{-8} \text{ m}^3$, where t is the injection time of the less viscous liquid). The value of Da is also shown. We measured the variations along x in the width of single fingers described in figure 17, normalized the width of the cell, which is denoted as w_f , where x is the coordinate in the finger propagation direction. The effects of Pe on w_f for cases (A)–(D) are shown in figure 18, while the effects of κ on w_f for various Pe are shown in figure 19. In the non-reactive case (A), significant effects of Pe on w_f are not observed in the range of Pe tested (figure 18a). In the reactive cases (B)–(D), significant effects of the reaction on w_f appear near the base. Figures 18(b–d) show that w_f near the base increases with a decrease in Pe (with an increase in Da) although w_f near the tip does not significantly vary with Pe . Figure 19 shows that w_f near the base increases with κ (with Da) for each Pe (although the difference by κ decreases with an increase in Pe), while w_f near the tip does not significantly vary with κ . These results in figures 18 and 19 are summarized in figure 20 in which w_f in the reactive cases are shown in terms of Da . In this figure, w_f in the cases with similar values of Da is drawn with the same colour. In each colour, Da is high in the order of the circle, triangle and square plots. The plots of the same colour roughly coincide, which shows that the shapes of the single finger depend on Da and are independent of Pe . Figure 20 shows again that the width of a single finger increases with Da near the base whereas do not significantly vary with Da near the tip. This can clearly verify our consideration regarding the effects of the present reaction on the single finger mentioned in the

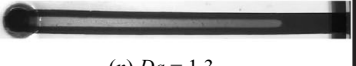
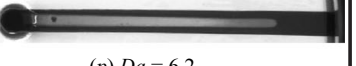
Pe	Case (A), $\kappa = 0$	Case (B), $\kappa = 0.011$	Case (C), $\kappa = 0.030$	Case (D), $\kappa = 0.049$
2.7×10^3	 (a) $Da = 0$	 (b) $Da = 13$	 (c) $Da = 38$	 (d) $Da = 62$
5.2×10^3	 (e) $Da = 0$	 (f) $Da = 6.8$	 (g) $Da = 20$	 (h) $Da = 32$
13×10^3	 (i) $Da = 0$	 (j) $Da = 2.6$	 (k) $Da = 7.6$	 (l) $Da = 12$
27×10^3	 (m) $Da = 0$	 (n) $Da = 1.3$	 (o) $Da = 3.8$	 (p) $Da = 6.2$

FIGURE 17. Single fingers for various Pe and for cases (A)–(D), where the amount of injected less viscous liquid is constant ($qt = 3.7 \times 10^{-8} \text{ m}^3$, where t is the injection time of the less viscous liquid). The value of Da is also shown. The injection time, t , is $t = 400, 200, 80$ and 40 s for $Pe = 2.7 \times 10^3$, $Pe = 5.2 \times 10^3$, $Pe = 13 \times 10^3$ and $Pe = 27 \times 10^3$, respectively.

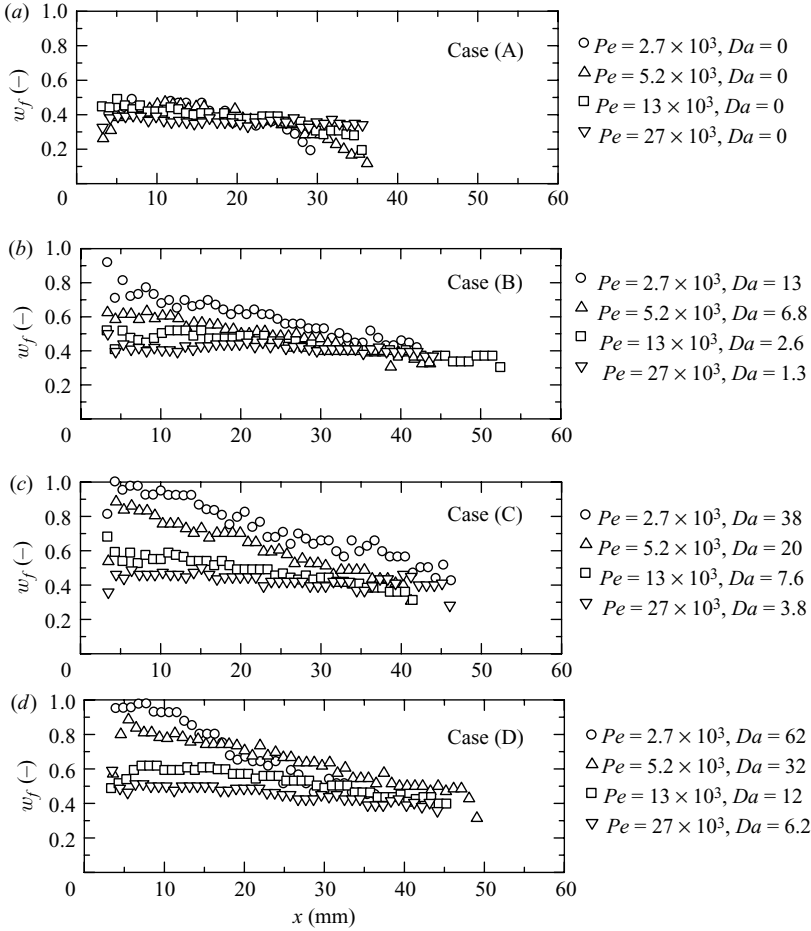


FIGURE 18. Effects of Pe on w_f for cases (A)–(D) regarding the single fingers shown in figure 17.

preceding section. It should be noted that figures 17–20 completely correspond to figures 5 and 7–9 in the radial case.

We measured the area density of the single finger within $x < 20$ mm, denoted as $d_{20,lin}$, which is the ratio of the area occupied by the single finger within $x < 20$ mm to the area of the cell within $x < 20$ mm, which is similar to d_{20} in figure 10 employed in the radial case. The results are shown in figure 21. As shown, $d_{20,lin}$ depends on the single parameter Da for various Pe and κ and increases with Da . This result is closely similar to that in the radial case shown in figure 10, although there is a main difference between the experiments in the radial and linear geometries where the velocity of the advancing finger in the radial case slows down during the experiment whereas that in the linear case is unchanged during the experiment (this means Da of the advancing finger decreases during the radial experiment, while Da of the single finger is unchanged during the linear experiment). The similarity between figures 10 and 21 suggests that the decrease in the velocity (or Da) of the advancing finger does not play an important role in the formation of the fingering pattern in the radial geometry.

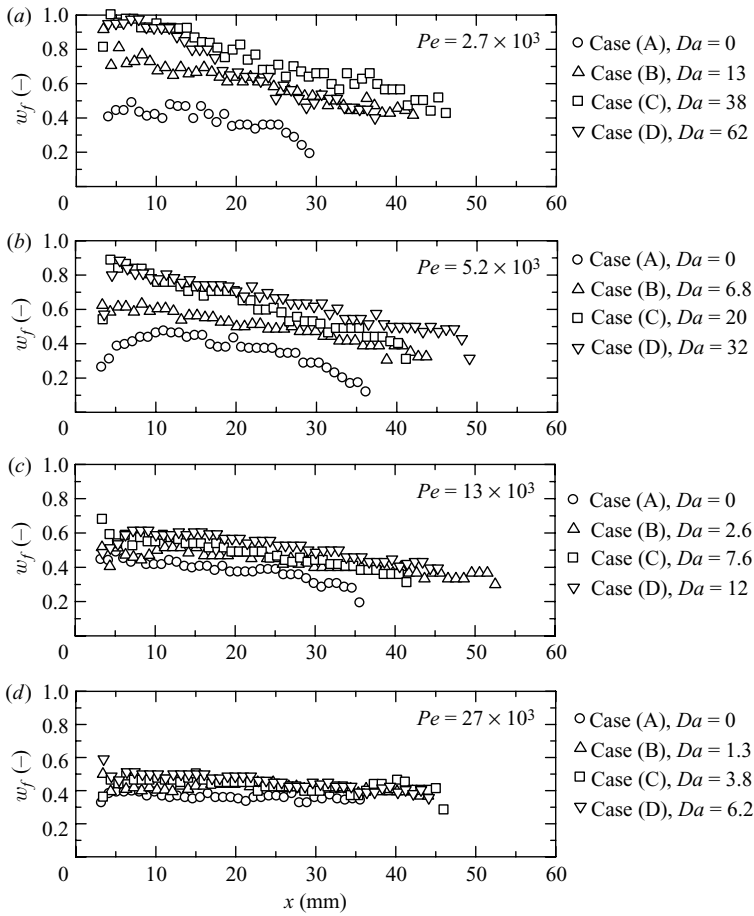


FIGURE 19. Effects of κ on w_f for various Pe regarding the single fingers shown in figure 17.

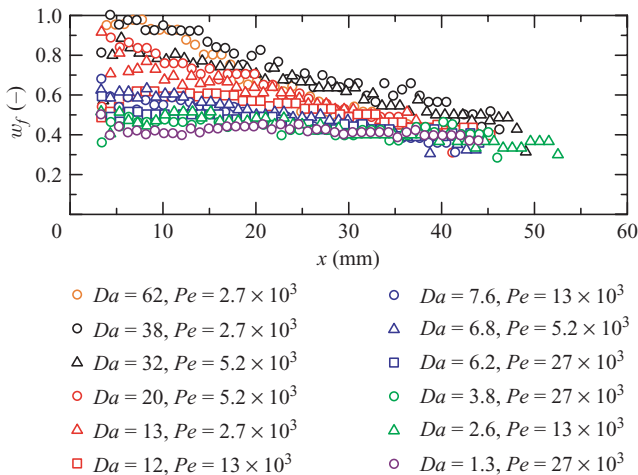


FIGURE 20. w_f for various values of Da regarding the single fingers shown in figure 17.

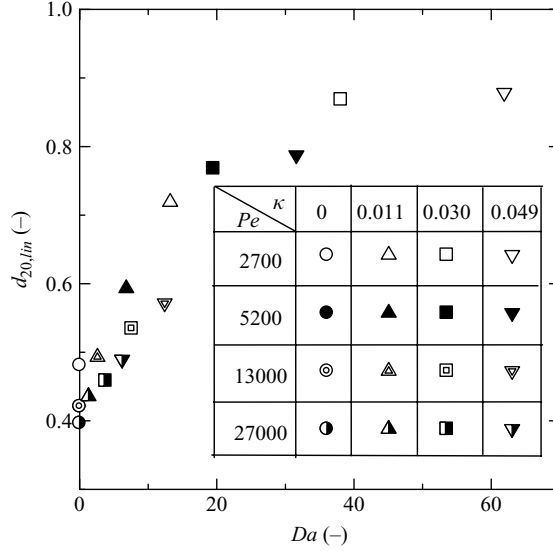


FIGURE 21. Relationship between $d_{20,lin}$ and Da regarding the single fingers shown in figure 17.

4. Discussion

In §3.3, we showed that the effects of the decrease in the viscosity of the more viscous liquid due to chemical reaction on the viscous fingering pattern for moderate Da are opposite to those for significantly high Da . In §3.4, we described that the present reaction involving moderate Da can be considered to widen a single finger mainly near the base. In §3.5, the consideration mentioned in §3.4 was verified by the single-finger experiments. This is clearly opposite to the case of significantly high Da , where the finger is narrowed by the reaction (Nagatsu *et al.* 2007). Here, we discuss the mechanism for the opposite effects depending on Da . In the case of significantly high Da , we hypothesized that an overall reaction rate is larger near the tip than near the base due to the larger amount of reactant flux provided near the tip. Thus, the viscosity of the more viscous liquid is relatively smaller near the tip than near the base. Since the displacing liquid can more easily penetrate the region with relatively lower viscosity than it can penetrate the region with relatively higher viscosity, the finger is narrowed. Note that this different selection mechanism of fingering due to anisotropy in the viscosity along the finger interface (or boundary) will be adapted regardless of the system being immiscible or miscible because it is based on a modification in the equation of motion. To discuss the case of moderate Da , we introduce a local Damköhler number (Da^*) based on the local fluid residence time, $t_{r,l}$, or the local finger advancement velocity, V , as

$$Da^* = \kappa t_{r,l} = \frac{\kappa R_0}{V}, \quad (4.1)$$

where $t_{r,l} = R_0/V$ (Fernandez & Homsy 2003). We can consider that V is higher near the tip than near the base or that $t_{r,l}$ is larger near the base than near the tip. This leads to Da^* being higher near the base than near the tip. Higher Da^* means higher completion of the reaction. This results in the viscosity of the more viscous liquid being relatively lower near the base than near the tip. This situation is contrary to that in the case of significantly high Da mentioned above. The displacing

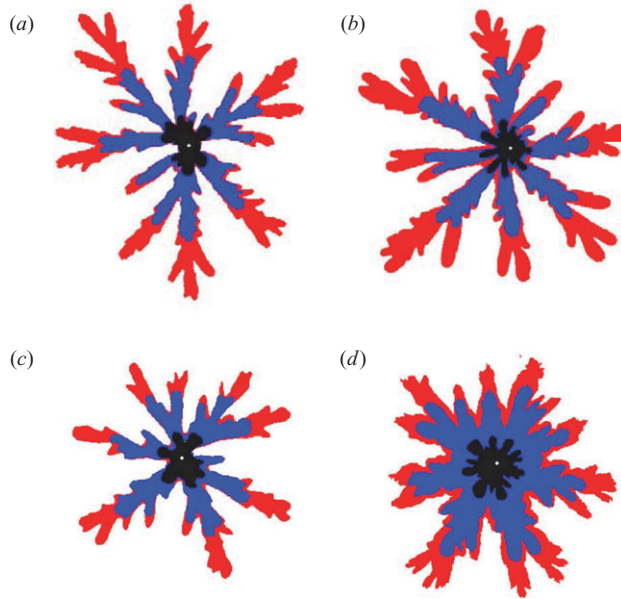


FIGURE 22. The overlays of the fingering patterns at several times shown (a) in figure 12(a), (b) in figure 12(b), (c) in figure 13(a) and (d) in figure 13(b). In (a) and (b), the fingering patterns at 10, 60 and 120 s are drawn in black, blue and red colours, respectively. In (c) and (d), the fingering patterns at 100, 600 and 1200 s are drawn in black, blue and red colours, respectively.

liquid penetrating more easily the region with relatively lower viscosity results in the finger being widened mainly near the base in the present case. This difference in viscosity distribution along the finger interface is the most plausible mechanism for the opposite effects depending on Da . It should be noted that there is difference between V or $t_{r,l}$ near the tip and that near the base even in the case of significantly high Da . In this case, however, there is no difference between Da^* near the tip and that near the base since κ can be treated as infinity.

Here, the overlays of the fingering patterns at several times shown in figures 12(a) and (b) are described in figures 22(a) and 22(b), respectively. In figure 22(a), the red colour at the finger base (around the injection hole) hardly appears, which shows that the finger width at the base hardly changes with time in the non-reactive case. This result is consistent with a known understanding that there is no interface velocity at the base, i.e. dynamics occurs only at the tip in the standard viscous fingering where the viscosity along the interface is not changed with time. In figure 22(b), in contrast, the red colour is observed at the base (around the injection hole), which shows that the finger width at the base increases with time in the reactive case. The comparison between the figures 22(a) and 22(b) verifies the mechanism for the formation of the present reactive finger proposed in the preceding paragraph in which the reactive finger base is widened over time. Figure 22(b) also suggests that the known understanding mentioned above is not applicable for the system in which the viscosity along the interface is locally changed with time by chemical reaction. Note that the results in figures 22(a) and 22(b) are also confirmed by the $d-r$ curves in figure 12(c) where the $d-r$ curves around the injection hole ($r < 20$ mm) in the non-reactive case hardly change with time, while that in the reactive case shift upward with time. The overlays of the fingering pattern at several times shown in figures 13(a) and 13(b)

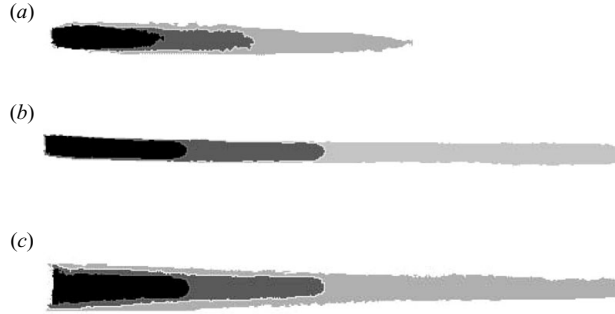


FIGURE 23. The overlays of the single fingers at several times shown (a) in figure 17(a), (b) in figure 17(o) and (c) in figure 17(c). In (a) and (c), the fingers at 100, 200 and 400 s are drawn in black, dark grey and light grey colours, respectively. In (b), the fingers at 10, 20 and 40 s are drawn in black, dark grey and light grey colours, respectively.

are also described in figures 22(c) and 22(d), respectively. In the non-reactive case, the red colour at the finger base is hardly observed in figure 22(c). In the reactive case in figure 22(d), the red colour at the finger base is observed. Comparing figure 22(d) with figure 22(b), we find that the extent of widening of finger base is more significant as Da is larger. Figures 23(a–c) describe the overlays of the single fingers at several times shown in figures 17(a) (the case of low Pe and $Da = 0$), (o) (high Pe and low Da), and (c) (low Pe and high Da), respectively. We can observe that the finger is significantly widened near the base for the high Da case (c), whereas the finger widening at the base is insignificant for the low Da case (b) or for the non-reactive case (a). These results show that the proposed mechanism for the formation of the present reactive finger can be verified by the single-finger experiments.

It should be noted that it is impossible to raise the concentration of the metal ions because of the limit to their solubility in the present system. If we find a system in which Da can be varied from a finite value to infinity (a significantly large value), the d_{max} with reaction will increase with Da up to a threshold value and decrease with Da over the threshold value and finally become smaller than that without reaction.

Here, we make further discussion regarding the finger widening near the base due to the present reaction by using a simplified model described in figure 24. The coordinates x and y are set in a single finger, where the direction x is that of finger propagation and $x = L$ means the tip of the finger (figure 24a). Now we assume that the local finger advancement velocity in the x direction, V_x , at an arbitrary position on the finger interface (x_i, y_i) is proportional to the length of the finger at the point (this equals to x_i) (figure 24b). For the previous system involving significantly high Da (Nagatsu *et al.* 2007), we can consider reactant flux to the interface in the x direction, F_x , at (x_i, y_i) is proportional to V_x and thus to x_i based on the assumption mentioned above (figure 24c). This leads to the product concentration c_p along the finger interface which is also proportional to x_i (figure 24c). We know that the viscosity of the more viscous liquid linearly increases with the product concentration in the previous system involving the viscosity increase (see the Appendix). As a result, the viscosity of the more viscous liquid at (x_i, y_i) in the previous system involving the viscosity increase, η_1 , satisfies the linear relation to x_i , as $\eta_1 = A_1 x_i + B_1$, where A_1 and B_1 are positive constants. For the present system, we can consider the local Damköhler number (Da^*) introduced earlier, which is proportional to x_i^{-1} based on the assumption mentioned above (figure 24d). Thus, the local fluid residence time,

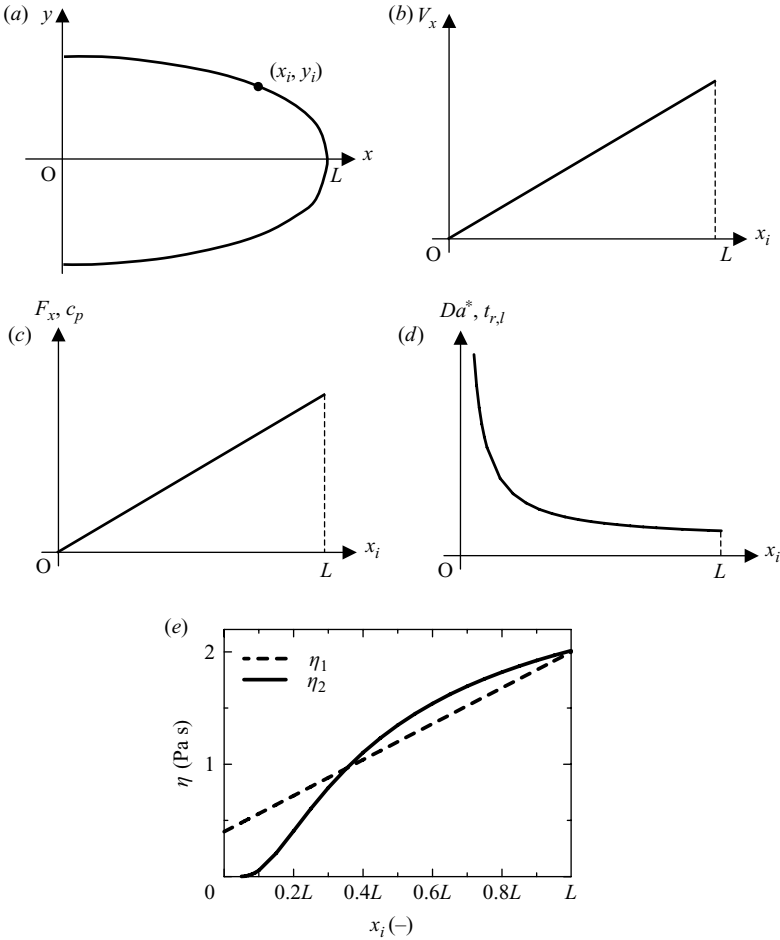


FIGURE 24. (a) Schematic of a single finger showing the definition of the coordinates and (x_i, y_i) at the finger interface. (b) Schematic of the relationship between V_x and x_i . (c) Schematic of the relationship between F_x or c_p and x_i for the previous system. (d) Schematic of the relationship between Da^* or $t_{r,l}$ and x_i for the present system. (e) Calculated η_1 and η_2 under the reasonable boundary conditions.

$t_{r,l}$, is also proportional to x_i^{-1} (figure 24d). In the present system, the viscosity of the more viscous liquid can be considered to exponentially decrease with time on the basis of the results shown in figure 3. We can consider that the viscosity of the more viscous liquid at (x_i, y_i) in the present system involving the viscosity decrease, η_2 , exponentially decreases with $t_{r,l}$ and is expressed as $\eta_2 = A_2 \exp(-B_2/x_i)$, where A_2 and B_2 are positive constants. Figure 24(e) shows η_1 and η_2 where the positive constants A_1, B_1, A_2 and B_2 are determined to satisfy boundary conditions such as $\eta_1 = \eta_2 = 2 \text{ Pa s}$ at $x = L$ and $\eta_1 = 0.4 \text{ Pa s}$ and $\eta_2 = 0.001 \text{ Pa s}$ at $x = 0.05L$. These boundary conditions are considered to be reasonable because the viscosity of the more viscous liquid under the condition of the shear rate being $\dot{\gamma} = 1 \text{ s}^{-1}$ in the previous system varied in the range of 0.4–2 Pa s (see the Appendix) and that in the present system varied in the range of 0.001–2 Pa s (see figure 4 and we noted that the viscosity of the more viscous liquid after the completion of the reaction became that of water). Figure 24(e) shows that in the region of $x_i < 0.35L$, $\eta_1 > \eta_2$,

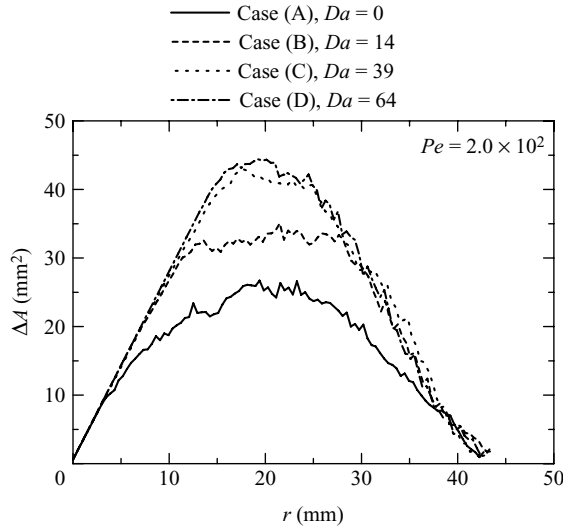


FIGURE 25. $\Delta A(r)$ as a function of r under the condition shown in figure 5 in which the total amount of the injected less viscous liquid is identical for $Pe = 2.0 \times 10^2$.

while in the region of $x_i > 0.35L$, $\eta_1 < \eta_2$. Based on the concept in which the displacing liquid penetrates more easily the region with relatively lower viscosity, this indicates that it is easier for the finger to be widened near the base in the present system than in the previous system. Also, it is more difficult to be widened near the tip in the present system than in the previous system. These results theoretically support that the finger is widened mainly near the base in the present system since the finger is considered to be totally widened in the previous system involving the viscosity increase.

Final discussion is made below. Figure 25 shows the $\Delta A(r) - r$ relation under the condition shown in figure 5 (where the total amount of the injected less viscous liquid is identical) for $Pe = 2.0 \times 10^2$, where Δr is set to 0.4 mm. Here, the $\Delta A(r) - r$ relation is described as curves rather than plots. In this figure, the area surrounded between the $\Delta A(r) - r$ curve and the horizontal axis equals to the total area of the fingering pattern. Under the same amount of the injected less viscous liquid, if there is no dispersion effect (this means immiscible system) and if the less viscous liquid completely displaces the more viscous liquid in the cell's gap direction (i.e. the fingering is completely two-dimensional in the $r - \theta$ plane), the total area will be the same for all cases. As shown in figure 25, however, the total area increases with Da although there is little difference in cases (C) and (D). We now consider that the more plausible reason of the difference in the total area is an increase in the dispersion effect accompanied by the decrease in the viscosity of the more viscous liquid due to the chemical reaction. This is because the significant difference in the area due to Da occurs mainly inside the pattern ($15 \text{ mm} < r < 30 \text{ mm}$), while the difference is less significant near the tip ($r > 30 \text{ mm}$) in figure 25. This suggests that the increase in the dispersion effects contributes to the increase in the area of the fingering pattern near the injection hole with Da .

5. Conclusion

In the present study, we found that a chemical reaction between a polyethylene oxide (PEO) solution and a solution containing copper ions Cu^{2+} and ferrous ions

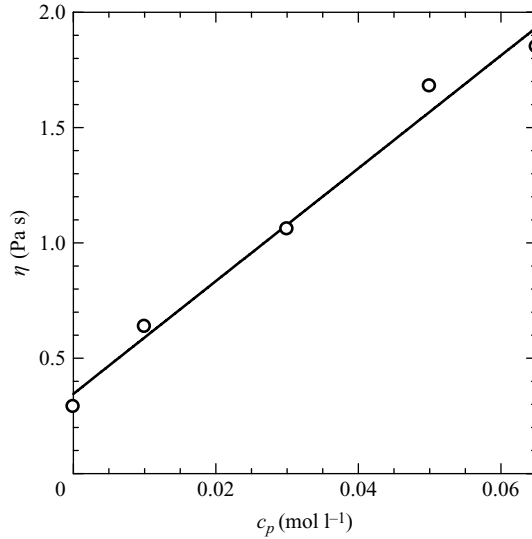


FIGURE 26. Dependence of viscosity of the more viscous liquid on the product concentration in the previous system involving the viscosity increase by the instantaneous reaction under the condition in which shear rate is $\dot{\gamma} = 1 \text{ s}^{-1}$.

Fe^{2+} decreases the viscosity of the mixture solution and that the concentration of the ions changes the rate of the decrease in viscosity, which corresponds to the chemical reaction rate, under the condition in which the rate is finite. We have succeeded in experimentally investigating the effects on miscible viscous fingering in Hele-Shaw cells of the decrease in the displaced liquid's viscosity due to chemical reaction under the condition where Pe and moderate Da are independently varied by using the PEO solution and the ionic solution as the more and less viscous liquids, respectively.

Main analysis has been done for the radial fingering. In the range of Pe employed here, the fingering patterns without the reaction ($Da = 0$) were independent of Pe . The fingering patterns with the reaction depended on the single parameter, Da , and the area occupied by the fingering pattern near the injection hole increased with Da in the range of Da employed here. The fractal dimension of the reactive fingering pattern also scaled on Da and increased with Da . This is consistent with the independence of the fingering patterns without the reaction on Pe . We also investigated the time evolution of the effects of the reaction on the fingering pattern. In the range of Da employed here, the significant influence of the reaction on the pattern appeared beginning in the later stage of the fingering for low Da and beginning in the middle stage for high Da . We measured the ratio of the area occupied by the fingering pattern within the circle whose radius is the longest finger's length to the area of the circle, d_{max} , as was done in the previous study by Nagatsu *et al.* (2007) in which d_{max} with the reaction decreasing the viscosity of the more viscous liquid involving significantly high Da was smaller than that without the reaction. In the range of Da employed here, d_{max} increased with Da . In other words, d_{max} with the reaction was larger than that without the reaction. This result is opposite to that in the previous case. Experiments in the linear geometry show that the shape of a single finger also depended on the single parameter, Da , and the finger width increased near the base with Da . This result is also opposite to that in the previous case in which the width of a single finger was considered to be decreased by the reaction. These results, interestingly, show that

the effects of the decrease in the viscosity of the more viscous liquid due to chemical reaction for moderate Da are opposite to those for significantly high Da . A mechanism for the opposite effects on the fingering pattern depending on Da is discussed.

The authors would like to thank Mr. Takehiko Arai, Eko Instrument Co., Ltd., for his help in measuring viscosity and the first normal stress difference of the polymer solutions. This research was partially supported by the Research Foundation for Electrotechnology of Chubu, Japan. The authors are also grateful to Professor Anne De Wit, Université Libre de Bruxelles, Belgium, for helpful discussion.

Appendix: Dependence of viscosity of the more viscous liquid on the product concentration in the previous system involving an increase in the viscosity by an instantaneous reaction (Nagatsu *et al.* 2007)

The reaction employed in the previous system involving an increase in the viscosity of the more viscous liquid by an instantaneous reaction was shown in (2.2) in Nagatsu *et al.* (2007). In the previous system, the viscosity increased with the product concentration, c_p , until c_p reached $c_p = 0.065 \text{ mol l}^{-1}$. Figure 26 shows the relationship between the viscosity of the more viscous liquid, η , and c_p under the condition in which shear rate is $\dot{\gamma} = 1 \text{ s}^{-1}$. As shown in figure 26, η linearly increases with c_p .

REFERENCES

- CHEN, J.-D. 1989 Growth of radial viscous fingers in a Hele-Shaw cell. *J. Fluid Mech.* **201**, 223–242.
- VAN DAMME, H., OBRECHT, F., LEVITZ, P., GATINEAU, L. & LAROCHE, C. 1986 Fractal viscous fingering in clay slurries. *Nature* **320**, 731–733.
- DEWIT, A. & HOMSY, G. M. 1999a Viscous fingering in reaction-diffusion systems. *J. Chem. Phys.* **110**, 8663–8675.
- DEWIT, A. & HOMSY, G. M. 1999b Nonlinear interaction of chemical reactions and viscous fingering in porous media. *Phys. Fluids* **11**, 949–951.
- FERNANDEZ, J. & HOMSY, G. M. 2003 Viscous fingering with chemical reaction: effect of in-situ production of surfactants. *J. Fluid Mech.* **480**, 267–281.
- HILL, S. 1952 Channeling in packed columns. *Chem. Engng Sci.* **1**, 247–253.
- HOMSY, G. M. 1987 Viscous fingering in porous media. *Ann. Rev. Fluid Mech.* **19**, 271–311.
- LEMAIRE E., LEVITZ P., DACCORD G. & VAN DAMME, H. 1991 From viscous fingering to viscoelastic fracturing in colloidal fluids. *Phys. Rev. Lett.* **67**, 2009–2012.
- LINDNER, A., BONN, D., CORVERA POIRÉ, E., BEN AMAR, M. & MEUNIER, J. 2002 Viscous fingering in non-Newtonian fluids. *J. Fluid Mech.* **469**, 237–256.
- LINDNER, A., BONN, D. & MEUNIER, J. 2000 Viscous fingering in a shear thinning fluid. *Phys. Fluids* **12**, 256–261.
- MCCLOUD, K. V. & MAHER, J. V. 1995 Experimental perturbations to Saffman–Taylor flow. *Phys. Rep.* **260**, 139–185.
- NAGATSU, Y., MATSUDA, K., KATO, Y. & TADA Y. 2007 Experimental study on miscible viscous fingering involving viscosity changes induced by variations in chemical species concentrations due to chemical reactions. *J. Fluid Mech.* **571**, 475–493.
- NITTMANN, J., DACCORD, G. & STANLEY, H. E. 1985 Fractal growth of viscous fingers: quantitative characterization of a fluid instability phenomenon. *Nature* **314**, 141–144.
- SAFFMAN, P. G. & TAYLOR, G. I. 1958 The penetration of a fluid into a porous medium or Hele-Shaw cell containing a more viscous liquid. *Proc. R. Soc. Lond. A* **245**, 312–329.
- TANVEER, S. 2000 Surprises in viscous fingering. *J. Fluid Mech.* **409**, 273–308.
- VICSEK, T. 1989 *Fractal Growth Phenomena*. World Scientific.
- VLAD, D. H. & MAHER, J. V. 2000 Tip-splitting instabilities in the Saffman–Taylor flow of constant viscosity elastic fluids. *Phys. Rev. E* **61**, 5439–5444.
- ZHAO, H. & MAHER, J. V. 1993 Associating-polymer effects in a Hele-Shaw experiment. *Phys. Rev. E* **47**, 4278–4283.